Published as: Fenton, O., Healy, M.G., Brennan, F.P., Thornton, S.F., Lanigan, G.J., Ibrahim, T.G. 2016. Holistic evaluation of field-scale denitrifying bioreactors as a basis to improve environmental quality. Journal of Environmental Quality 45(3): 788 – 795.
doi:10.2134/jeq2015.10.0500

O. Fenton[1], M.G. Healy[2], F.P. Brennan[3], S.F. Thornton[4], G.J. Lanigan[1], T.G. Ibrahim[1]

[1]Teagasc, Environment Research Centre, Johnstown Castle, Wexford, Co. Wexford, Ireland

[2]Civil Engineering, National University of Ireland, Galway, Co. Galway, Ireland

[3]Microbiology, National University of Ireland, Galway, Co. Galway, Ireland

[4]Groundwater Protection and Restoration Group, Kroto Research Institute, University of Sheffield, UK

*Corresponding author. Tel: +353 91 71271. E-mail address: owen.fenton@teagasc.ie

Abbreviations:

sustainability index (SI)

dissolved reactive phosphorus (DRP)

greenhouse gas (GHG)

dissolved organic carbon (DOC)

particulate nitrogen (PN)

total organic carbon (TOC)

maximum admissible concentration (MAC)

total dissolved nitrogen (TDN)

woodchip (WC)

sandy loam soil (SLS)

global warming potential (GWP)

dissimilatory nitrate reduction to ammonium (DNRA)

weighting factor (WF)

hydraulic loading rate (HLR)

Abstract

Denitrifying bioreactors effectively convert nitrate-nitrogen (NO_3-N) to di-nitrogen and thereby protect water quality in agricultural landscapes. In the present study, the performance of a pilot-scale bioreactor (50 m long, 5 m wide and 2 m deep) containing seven alternating cells, filled with either sandy loam soil or lodgepole pine woodchip, and with a novel zig-zag flow pattern, was investigated. The influent water had an average NO_3-N concentration of 25 mg L^{-1}. The performance of the bioreactor was evaluated in two scenarios. In scenario 1, only NO_3-N removal was evaluated, whereas in scenario 2, NO_3-N removal, ammonium-N (NH_4-N) and dissolved reactive phosphorus (DRP) generation was considered. These data were used to generate a 'sustainability index' (SI) – a number which evaluated the overall performance taking these parameters into account. When the bioreactor performance was evaluated in scenario 1, it was a net reducer of contaminants, but it transformed into a net producer of contaminants in scenario 2. Inquisition of the data using these scenarios meant that an optimum bioreactor design could be identified. This would involve the reduction of the filter length such that it comprised only two cells – a single sandy loam soil cell, followed by a woodchip cell, which would remove NO_3-N, reduce greenhouse gas (GHG) emissions and DRP losses. An additional post-bed chamber containing media to eliminate NH_4-N may be added to this bioreactor. Scenario modelling such as that proposed in this paper, should ideally include GHG in the SI, but as different countries have different emission targets, future work should concentrate on the development of geographically appropriate weightings to facilitate the incorporation of GHG into a SI.

Keywords: denitrifying bioreactor; sustainability index; greenhouse gas; nitrate.

54

55 Introduction

56 A denitrifying bioreactor is an artificial nitrogen (N) sink in which an organic carbon (C)
57 source (e.g. woodchip (WC)) is used to reduce nitrate (NO_3) in surface/subsurface drainage
58 or groundwater flow systems (Cameron and Schipper, 2010). Research on denitrifying
59 bioreactors (Schipper et al., 2010; Christianson et al., 2011) has focused on NO_3 removal,
60 despite the fact that anthropogenic activities such as agriculture produce NO_3, as well as a
61 range of other pollutants. Moreover, biophysical and biogeochemical processes occurring
62 within denitrifying bioreactors frequently generate other contaminants such as nitrous oxide
63 (N_2O), ammonia (NH_3), carbon dioxide (CO_2) and methane (CH_4), through 'pollution
64 swapping' (Fenton et al., 2014). This issue has been discussed in the literature (e.g. Grennan
65 et al., 2009; Elgood et al., 2010; Schipper et al., 2010; Woli et al., 2010; Shih et al., 2011;
66 Warneke et al., 2011; Healy et al., 2012; 2014), but denitrifying bioreactors designed to
67 control pollution swapping, such as permeable reactive interceptors, have only been
68 examined at laboratory-scale (Fenton et al., 2014; Ibrahim et al., 2015).

69

70 Fenton et al. (2014) proposed that denitrifying bioreactors should be analyzed holistically,
71 taking all losses into account. They presented a sustainability index (SI), using inlet and
72 outlet data, which identifies the "losses" in the system. Positive and negative balances of each
73 parameter indicate either removal or production of the parameter of interest. This analysis
74 indicates which parameters require additional interventions for the system to be
75 environmentally sustainable. Complete removal of nutrients without pollution swapping is
76 the ultimate goal, but thresholds imposed by environmental legislation may not be so
77 stringent. Therefore, a SI may be developed for various scenarios, taking water, gaseous
78 emissions, or both, into account. Healy et al. (2014) adopted this method of analysis in the

evaluation of laboratory denitrifying bioreactors containing various C-rich media, and found that the SI varied depending on the scenario examined. Analyzing NO_3 only, there was a net removal in the bioreactors. When all measured water quality parameters (NO_3, ammonium (NH_4) and dissolved reactive phosphorus (DRP)) were taken into account, there was a net release of contaminants from all bioreactors, which substantially increased when greenhouse gases (GHG) were included in the analysis.

The objectives of this study were: (1) to investigate this method of analysis at a much larger scale using a novel outdoor, pilot-scale denitrifying bioreactor (2) to illustrate how a SI and may be used to develop a permeable reactive interceptor, which minimizes pollution swapping.

Material and Methods

Denitrifying bioreactor design

A concrete tank (10 m long × 5 m wide × 2 m deep), with internally flanged 0.2 m-deep base panels, was laid on a concrete plinth (Fig. 1). The base of the tank was lined with heterogeneous clay textured soil. Non-reactive, high density polyethylene plastic sheets were sealed into the clay liner to create seven equally sized cells. The plastic sheets were positioned such that solute migration was forced into a zig-zag pattern to increase the hydraulic retention time, although dead zones were inevitably created. The cells in the tank were filled with either lodgepole pine woodchip (WC1-3) or sandy loam soil (SLS) (SLS1-4) (Fig. 1). Water was pumped into the tank and discharged from the denitrifying bioreactor outlet into an artificial drainage system.

Media preparation, characterization and installation

104 The WC used had a particle size ranging from 10 to 50 mm. Healy et al. (2012, 2014) and
105 Ibrahim et al. (2015) observed high dissolved organic carbon (DOC) effluent concentrations
106 in the early stages of operation of a denitrifying bioreactor. Therefore, prior to placement in
107 the pilot-scale bioreactor, the WC was spread in a uniform layer (10 long × 5 wide × 0.2 m
108 deep) in a clean, concrete holding area and regularly power-hosed using a mains water supply
109 over nine days. To determine potential losses from the media cells and the clay liner, samples
110 were tested for total N (TN) and total C (TC) using a thermal conductivity detector, following
111 combustion and separation in a chromatographic column, and the total P (TP) content was
112 determined by inductively coupled plasma emission spectroscopy (ICP-ES) after aqua regia
113 digestion.
114
115 Water, dissolved gas and surface emission instrumentation and monitoring
116 The SI was conducted using inlet/outlet data, whereas the provenance of losses within the
117 bioreactor was measured using nests of multi-level piezometers (inner diameter 0.05 m),
118 installed at 12 positions within the denitrifying bioreactor (Fig. 1). Each nest had sampling
119 ports at 0.1 m, 0.4 and 0.7 m below the surface. A fully screened piezometer, through which
120 influent water was injected into the denitrifying bioreactor, was installed in SLS1 (Fig. 1). In
121 each nest, gas impermeable tubing, with an inner diameter of 5 mm, was installed to the
122 center of the screen interval. At the surface level, a three-way stop cock and 50 ml-capacity
123 syringe (Fenton et al., 2011) was used to extract multi-level water and dissolved gas samples.
124
125 The denitrifying bioreactor was saturated, and influent potable mains water was pumped
126 continuously from a storage compartment (Fig. 1) into position 0 from August 2011, at a rate
127 of 0.2 to 0.3 m^3 d^{-1}. The characteristics of the mains water are shown in Table 1. Water
128 temperature in the denitrifying bioreactor was typically between 12 -14^{o}C at all depths, the

pH was 6.3-7.2, and the electrical conductivity (EC) was 229-820 µS cm^{-1}. On March 22, 2012 (210 days after the start of operation), the NO_3-N concentration of the influent water was modified to a target concentration of 25 mg L^{-1}, by adding potassium nitrate (KNO_3) salt in the storage compartment and mixing thoroughly. This target influent concentration was maintained until the end of the study (August 2012). The outlet was another fully screened piezometer positioned at position 12 (SLS4; Fig 1).

Water samples were collected from the inlet and outlet, and from all nests (longitudinal and vertical profiles), over a 5-month period (February to August 2012, 14 sampling dates). Water samples were collected in 50 ml polyethylene screw top bottles. Unfiltered and filtered samples (0.45 µm filter membrane) were collected. Nitrate-N, NH_4-N, dissolved organic nitrogen (DON), particulate nitrogen (PN), DRP and dissolved unreactive P (DUP) were analyzed on a Thermo Konelab 20 analyzer (Technical Lab Services, Ontario, Canada). Dissolved Organic Carbon (DOC) concentrations were analyzed on a TOC analyzer (TOC-V series, Shimadzu, Kyoto, Japan). pH, EC (µS cm^{-1}), temperature (^oC) and oxidation redox potential (ORP) were measured using a multi-parameter Troll 9500 probe (In situ, CO, U.S.A.) with a flow-through cell.

Triplicate water samples were collected for all sampling events to identify potential denitrification in the screened interval of each piezometer, based on dissolved N_2 and the N_2/argon (Ar) ratio (Kana et al., 1998). The samples were transferred from the syringe to a 12 ml Exetainer® (Labco Ltd., U.K.), filled from the base of each container, overfilled, and then sealed with a butyl rubber septum to avoid any air entrapment. Samples were then placed upside down under water (below the average groundwater temperature of 12^oC) in an ice box, transported to the laboratory, and kept in a dark cold room at 4^oC prior to analysis. Dissolved

154 N_2 and Ar were analyzed using membrane inlet mass spectrometry at groundwater
155 temperature (Kana et al., 1998).
156
157 To analyze dissolved gases (presented as N_2O-N, CO_2-C and CH_4-C), water samples were
158 collected periodically in 160-ml glass serum bottles. The bottles were capped and evacuated
159 prior to the sampling. Twenty ml of sample water was injected into the bottles, and then
160 helium gas was filled to bring back to atmospheric pressure. After equilibration, the head
161 space was sampled and analyzed by gas chromatography equipped with an electron capture
162 detector (N_2O-N analysis), a flame ionization detector (CH_4-C analysis) and a thermal
163 conductivity detector (CO_2-C analysis) (CP-3800, Varian, Inc. USA) using Ar as a carrier gas
164 (Jahangir et al., 2013).
165
166 Greenhouse gases from the bioreactor surface were measured using the static chamber
167 method (Hutchinson and Mosier, 1981; Smith and Dobbie, 2001). Chambers consisted of a
168 stainless steel structure with two components, a collar base (0.41 m × 0.41 m), and a lid (0.41
169 m × 0.41 m × 0.41 m), with a volume of 0.068 m^3 above ground level. To provide a gas-tight
170 seal, the collar base was filled with water. Chamber position was as in Fig. 1. Twenty ml
171 samples were drawn through a rubber septum (Becton Dickinson, UK) 20 min and one hour
172 after closure (Becton Dickinson, UK) using a 20 ml polypropylene syringe with a
173 hypodermic needle (BD Microlance 3, Becton Dickinson, UK) and injected into pre-
174 evacuated 7 ml screw-cap septum glass vials (Labco, UK). Gas concentration was quantified
175 using gas chromatography (see above). As fluxes are calculated from gas accumulation
176 within the chamber over time, samples were collected at four time-points per chamber (0, 15,
177 30 and 45 min after lid closure).
178

179 Sustainability Index and Damage Cost Approach

180 All parameters are expressed in g m^{-2} (of bioreactor surface area) d^{-1}. A SI is then created by
181 summation of all parameters (Fenton et al. 2014):

182

183 $$SI = a(B_{N_2O}) + b(B_{NO_3^-}) + c(B_{CH_4}) + d(B_{CO_2}) + etc..... \quad [1]$$

184

185 where B_x denotes the net loss (either positive or negative) of a specific contaminant from the
186 denitrifying bioreactor, and *a, b, c*, etc. are weighting factors (WF) that depend on the context
187 of the analysis (e.g. legislative, environmental, geographical). The rationale of Fenton et al.
188 (2014) was used to calculate the WFs. In the current study, two scenarios are examined. For
189 scenario 1, in countries or geographical areas where only NO_3-N concentration is considered,
190 the WF for NO_3 is set to 1, while the other measured parameters are set to zero. For scenario
191 2, in which NO_3-N, NH_4-N and DRP are considered, the maximum admissible concentration
192 (MAC) for these parameters is used to determine the WFs. In Ireland, for example, the MAC
193 for molybdate-reactive P (MRP = DRP in the current study) and NH_4-N in rivers is 35 μg L^{-1}
194 and 65 μg L^{-1}, respectively, while NO_3-N in estuaries should not exceed 2.5 mg L^{-1}
195 (Bowman, 2009). As DRP is the most sensitive parameter in this scenario, the WFs for DRP,
196 NH_4-N and NO_3-N are set to 1, 0.538 (35/65) and 0.014 (35/2500), respectively. Calculating
197 a WF for GHGs is more problematic, as there is no MAC for GHGs and, moreover,
198 individual countries have very different targets in terms of their GHG commitments. For
199 example, under the EU 2020 Climate and Energy Package (EC, 2012), the Republic of
200 Ireland must reduce GHG emissions by 20% by 2020, whereas developing countries, such as
201 China and India, have no international commitments in terms of emissions reduction. As a
202 result, the WF for GHG used in the SI should reflect the relative importance of GHG limits in

203 terms of national policy objectives, and be set at a level that is nationally appropriate in terms
204 of policy relative to other pollutants.
205
206 A damage cost approach was also used, which assigned a cost to each of the water quality
207 and GHG parameters examined in terms of damage to the environment and human health
208 (Eory et al., 2013; Anon, 2014). For the water parameters, the costs per tonne (converting
209 from pounds sterling to euro at the time of writing) were €916 (NO_3-N), €61553 (P) and
210 €2458 (NH_4-N) (Eory et al., 2013). A cost per year was assigned to scenarios 1 and 2 by
211 substituting the unit costs for each pollutant as WFs in Eqn. 1. These values were multiplied
212 by 365 to give yearly equivalents.
213
214 Results and Discussion
215 Media and woodchip washing
216 The WC had higher TN content than the clay liner and SLS cells (Table 2). However, the TP
217 of the clay liner, WC and SLS were low, and were reflective of P-deficient agronomic
218 grassland soils. In previous studies (Healy et al., 2014), there were considerable C, N and P
219 losses from bioreactors immediately after the start of operation. In the current study, the
220 concentrations of the NH_4-N and DRP concentrations in the drainage water decreased from
221 ~7 to <1 mg L^{-1} over the two washing periods, but were still relatively high, considering the
222 TP content of the WC. This suggests that washing of the WC prior to installation in the
223 bioreactor is an efficient means of reducing losses.
224
225 Carbon, Nitrogen and Phosphorus
226 The DOC and dissolved CH_4-C concentrations were higher at the outlet than at the inlet of
227 the denitrifying bioreactor (Fig. 2), and were highest in deep flow paths (Fig. 3), as a result of

prolonged interaction of water with the woodchip media. The highest dissolved CO_2-C and CH_4-C concentrations (501 and 26 mg L^{-1}, respectively, Fig. 3) were measured in deep flow paths, which is indicative of lower redox conditions at this depth.

Water temperature in the denitrifying bioreactor was typically between 12-14 ºC at all depths, with pH ranging from 6.3 to 7.2, and EC ranging from 229 to 820 µS cm^{-1}. Nitrate-N and DON concentrations were reduced within the denitrifying bioreactor, but NH_4-N concentrations were higher at the outlet (Fig. 4). Most of the reduction of the NO_3-N occurred in SLS1 and WC1 of the bioreactor (Fig. 5). It was also in these cells also that the highest N_2/Ar (55 at the outlet of WC1; Fig. 5) and dissolved N_2O-N concentrations (1000 µg L^{-1} at the outlet of WC1; Fig. 5) were measured. This probably indicates that partial and full heterotrophic denitrification occurred in these two cells, as a result of bioavailable DOC, a sufficient supply of O_2 for N_2O formation, and short water transit-times. Dissolved organic nitrogen concentrations increased from below detection to a maximum of 10 mg L^{-1} after amendment of the inlet water with KNO_3, but remained below 0.9 mg L^{-1} at the outlet for the entire study period (Fig. 4). Longitudinal patterns in the ORP decreased from positive values in SLS1 to negative values in WC3, but increased in SLS2 (maximum increase of -121 to 111 mV) (data not shown).

In WC2, SLS3 and WC3 (sampling points 6 – 12), NO_3-N concentrations were below detection, while N_2/Ar and dissolved N_2O-N concentrations decreased (Fig. 5). After modification with KNO_3, NH_4-N generally increased from inlet to outlet (Fig. 5), and the highest concentrations were observed in the deep water flow paths.

In Warneke et al. (2011) NH_4 ranged from <0.0007 mg L^{-1} to 2.12 mg L^{-1} and NO_2 concentrations ranged from 0.0018 mg L^{-1} to 0.95 mg L^{-1}. Such concentrations were thought not to infer anammox as a likely mechanism for NO_3 removal in the denitrification bed. The increase in NH_4 has several plausible origins. These include dissimilatory nitrate reduction to ammonium (DNRA), suggested by Healy et al. (2014) to occur in denitrifying bioreactors where the media has a high C/N ratio (e.g. >12). DNRA is also energetically favored over denitrification in reducing conditions, where NO_3 becomes limited as an electron acceptor. Such a process is known to occur in artificially drained fields, where heavy textured soil with moderate permeability enables transformation to NH_4 from NO_3 (Necpalova et al., 2012). An alternative is ammonification of organic N compounds in the woodchip and release to the fluid phase, which is supported by corresponding increases in P. Such processes, together with the release of NH_4 from the SLS and WC, may contribute to an increase in NH_4-N concentrations. In the present study much of the NH_4 stems from within the bioreactor, illustrated by the high levels of NH_4 when compared with NO_3 in the pre-spike phase. This correlates well with the methane production, which could be a product of anaerobic N mineralization. However, in terms of removal of NO_3 when concentrations begin to drop, we propose that DNRA would be favored over NO_3 immobilization as given a choice, microbes preferentially use NH_4 over NO_3 for growth, as it is much more energy efficient to do so.

Before installation, washing of the woodchip media showed consistently high release of DRP concentrations. Over the entire study period, DRP, DUP and PP concentrations were higher at the outlet than the inlet (Fig. 4), but these concentrations decreased over time. The longitudinal data indicates that the WC cells (WC1and WC2) were the source of DRP (Fig. 5). In addition, the heterogeneous clay liner, given its relatively high P content (Table 2), could have contributed to the P loss at specific locations.

277

278 Greenhouse gas emissions to the atmosphere

279 The N_2O-N (Fig. 6) emissions were greater in the first three cells (maximum N_2O-N emission
280 of 70.0 mg N_2O-N m^{-2} d^{-1} in WC1), and were likely linked to partial denitrification. This also
281 indicated that anoxic, as opposed to anaerobic conditions, prevailed in these cells. In contrast,
282 CH_4-C and CO_2-C emissions (Fig. 6) peaked towards the outlet of the denitrifying bioreactor,
283 and were linked to lower ORP at this position. Warneke et al. (2011) measured average
284 surface emissions of N_2O-N and CO_2-C of 79 μg m^{-2} min^{-1} (or 113.2 mg m^{-2} d^{-1}, comparable
285 to current study) (reflecting 1% of the removed NO_3-N) and 12.6 mg m^{-2} min^{-1}, respectively.
286 Observed methane emissions were considerably higher than those reported for stream bed
287 denitrifying bioreactors containing woodchip (Elgood et al., 2010), but were on a par with
288 emissions from column studies (Healy et al., 2012) and indeed were in the lower range of
289 values reported for landfill systems (Chanton and Liptay, 2000).

290

291 Conversion to a permeable reactive interceptor

292 The SIs calculated for the entire bioreactor are presented in Table 3. In scenario 1, where
293 NO_3-N only was considered, the denitrifying bioreactor was successful in remediating NO_3-N
294 (SI of 0.121 g m^{-2} d^{-1}). This is comparable to SIs calculated for laboratory denitrifying
295 bioreactors containing various C-rich media, in which SIs of between 0.81 and 1.46 g $m^{-2}d^{-1}$
296 were measured (Healy et al., 2014). However, when other water quality parameters (scenario
297 2) were factored in, similar to Healy et al. (2014), the denitrifying bioreactor transformed
298 from a net reducer of contaminants to a net producer of contaminants (SI of – 0.00011 g $m^{-2}d^{-}$
299 ^{1}; Table 3).

300

301 SLS1 and WC1 of the denitrifying bioreactor (Fig 1) were successful in removing NO_3, but
302 were also sources of other contaminants of NH_4 and GHGs. While these contaminants did not
303 peak until the influent water reached the subsequent cells, the longitudinal data collected
304 from the bioreactor (Figs 3, 5 and 6), combined with the calculated SIs (Table 3), suggest that
305 the present unit could be converted to a permeable reactive interceptor (Fenton et al., 2014)
306 by reduction to three cells: the existing first two cells (SLS1, WC1), followed by a post bed
307 cell containing media, such as zeolite, which would be capable of reducing NH_4, thereby
308 mitigating DRP and GHG emissions caused by bioreactor P losses and N limitation further on
309 in the bioreactor. The likely DRP losses requiring sequestration from inlet DRP will be small,
310 as indicative drainage DRP concentrations in the vicinity are < 0.01 mg/L. The performance
311 of this new configuration could then be assessed by performing a new SI calculation. Re-
312 calculating the SI based on this smaller configuration gives 0.112 and -0.002, for Scenarios 1
313 and 2, respectively.
314
315 Recommendations for the future
316 It should be noted that while the idea of understanding pollution swapping is of course
317 important, the precise nature of the input variables/weighting needs to be developed further.
318 A consensus needs to be reached across the research community which reflects different
319 scenarios. The SI is context-specific and dependent upon the selected weighting factors,
320 which, in turn, should be informed by national and international environmental policy
321 priorities.
322
323 Important considerations for the future when using this approach are cost and time. In this
324 study, each sampling event lasted four days, and a team of three people were needed in the
325 field to complete all the multilevel piezometer and multi-parameter sampling. In addition to

training costs of the personnel, consumable, labor and analysis costs were extensive (total costs were in excess of €40,000 over the total study duration). Of course, such costs are associated with intense analyses required for a research project. On a commercial farm site, the dimensions and monitoring system will inevitably vary and therefore costs will be lowered. Depending on the parameters analyzed, a denitrifying bioreactor may either negate costs (if only water quality parameters are measured) or cause damage to the environment (particularly if GHG emissions are considered) (Table 3). When modifying a denitrifying bioreactor to a permeable reactive interceptor to reduce contaminant losses (e.g. reduction of N_2O losses thereby eliminating indirect losses from NO_3 leaching), the cost of environmental damage should also be considered within a life cycle analysis. This will also allow easy comparison with other systems.

Acknowledgments

The authors acknowledge funding from the Department of Agriculture, Forestry and the Marine (DAFM) Research Stimulus Fund (Project number: RSF 07 525) and the Teagasc Post-Doctoral fund.

351 References

352 Anon. 2014. Valuation of energy use and greenhouse gas (GHG) emissions.
353 Supplementary guidance to the HM Treasury Green Book on Appraisal and Evaluation in
354 Central Government. September 2014. Department of Energy and Climate Change, UK.
355 https://www.gov.uk/government/uploads/system/uploads/attachment_data/file/360316/20141
356 001_2014_DECC_HMT_Supplementary_Appraisal_Guidance.pdf

357 Bowman, J. 2009. New water framework directive environmental quality standards
358 and biological and hydromorphological classification systems for surface waters in Ireland.
359 Biol. Env : Proced. Royal Ir. Acad. 109B(3) : 247 – 260.

360 Cameron, S.C., and L.A. Schipper. 2010. Nitrate removal and hydraulic performance
361 of carbon substrates for potential use in denitrification beds. Ecol. Eng. 36 (11):1588–1595.

362 Chanton, J.P., Liptay, K., 2000. Seasonal variation in methane oxidation in a landfill
363 cover soil as determined by an in situ stable isotope technique. Global Biogeochem. Cycle
364 14:51–60.

365 Christianson, L.E., J.A. Hanly, and M.J. Hedley. 2011. Optimized denitrification
366 bioreactor treatment through simulated drainage containment. Agric. Water Manage. 99:85–
367 92.

368 European Commission. 2012. Analysis of options beyond 20% GHG emission
369 reductions: member state results.
370 http://ec.europa.eu/clima/policies/strategies/2020/docs/swd_2012_5_en.pdf

371 Elgood, Z., W.D. Robertson, S.L. Schiff, and R. Elgood. 2010. Nitrate removal and
372 greenhouse gas production in a stream-bed denitrifying bioreactor. Ecol. Eng. 36:1575–1580.

373 Eory, V. C.F.E. Topp, and D. Moran. 2013. Multiple-pollutant cost-effectiveness of
374 greenhouse gas mitigation measures in the UK agriculture. Environ. Sci. Policy, 27:55-67.

375 Fenton, O., M.G. Healy, T. Henry, M.I. Khalil, J. Grant, A. Baily, and K.G. Richards.
376 2011. Exploring the relationship between groundwater geochemical factors and
377 denitrification potentials on a dairy farm in south east Ireland. Ecol. Eng. 37: 1304–1313.
378 Fenton, O., K.G. Richards, S. Thornton, F. Brennan, M.G. Healy, M.M.R. Jahangir,
379 and T.G. Ibrahim. 2014. Permeable reactive interceptors – blocking diffuse nutrient and
380 greenhouse gas losses in key areas of the farming landscape. J Agri. Sci. 152:S71–S81.
381 Grennan, C.M., Moorman, T.B., Parkin, T.B., Kaspar, T.C., Jaynes, D.B., 2009.
382 Denitrification in wood chip bioreactors at different water flows. Journal of Environmental
383 Quality 38 (4), 1664 – 1671.
384 Healy, M.G., T.G. Ibrahim, G.J. Lanigan, A. João Serrenho, and O. Fenton. 2012.
385 Nitrate removal rate, efficiency and pollution swapping potential of different organic media
386 in laboratory denitrification bioreactors. Ecol. Eng. 40:198–209
387 Healy, M. G., M. Barrett, G.J. Lanigan, A. João Serrenho, T.G. Ibrahim, S. Thornton,
388 S.A. Rolfe, W.E. Huang, and O. Fenton. 2014. Optimizing nitrate removal and evaluating
389 pollution swapping trade-offs from laboratory denitrification bioreactors. Ecol. Eng. 74:290–
390 301.
391 Hutchinson, G.L., and A.R. Mosier. 1981. Improved soil cover method for field
392 measurement of nitrous oxide fluxes. Soil Sci. Soc. Am. J. 45:311–316.
393 Ibrahim, T.G., A. Goutelle, M.G. Healy, R. Brennan, P. Tuohy, J. Humphreys, G.J.
394 Lanigan, J. Brechignac, and O. Fenton. 2015. Mixed Agricultural Pollutant Mitigation Using
395 Woodchip/Pea Gravel and Woodchip/Zeolite Permeable Reactive Interceptors. Water Soil
396 and Air Pol. 226:51– DOI 10.1007/s11270-015-2335-4
397 Jahangir, M.M.R., Johnston, P., Barrett, M., Khalil, M.I., Groffman, P., Boeckx, P.,
398 Fenton, O., Murphy, J., Richards, K.G., 2013. Denitrification and indirect N_2O emissions in
399 groundwater: hydrologic and biogeochemical influences. J. Contam. Hydrol. 152:70–81.

400 Kana, T.M., M.B. Sullivan, J.C. Cornwell, and K. Groszkowski. 1998. Denitrification
401 in estuarine sediments determined by membrane inlet mass spectrometry. Limnol. Oceanogr.
402 43(2):334–339.

403 Necpalova, M., O. Fenton, I. Casey, and J. Humphreys. 2012. N leaching to
404 groundwater from dairy production involving grazing over the winter on a clay-loam soil.
405 Sci. Tot. Environ. 432:159–172.

406 Schipper, L.A., W.D. Robertson, A.J. Gold, D.B. Jaynes, and S.C. Cameron. 2010.
407 Denitrifying bioreactors: An approach for reducing nitrate loads to receiving waters. Ecol.
408 Eng. 36:1532–1543.

409 Shih, R., W.D. Robertson, S.L. Schiff, and D.L. Ruldolph. 2011. Nitrate controls
410 methyl mercury production in a streambed bioreactor. J. Environ. Qual. 40:1586–1592.

411 Smith, K.A., and K.E. Dobbie. 2001. The impact of sampling frequency and sampling
412 times on chamber-based measurements of N_2O emissions from fertilized soils. Global
413 Change Biol. 7:933–945.

414 Warneke, S., L.A. Schipper, D.A. Breuswitz, I. McDonald, and S. Cameron. 2011.
415 Rates, controls and potential adverse effects of nitrate removal in a denitrification bed. Ecol.
416 Eng. 37:511–522.

417 Woli, K.P., M.B. David, R.A. Cooke, G.F. McIsaac, and C.A. Mitchell. 2010.
418 Nitrogen balance in and export from agricultural fields associated with controlled drainage
419 systems and denitrifying bioreactors. Ecol. Eng. 36:1558–1566.

420

421

422 Captions for Figures

423 Fig. 1 Schematic top view of the denitrifying bioreactor (top). Cross section of the tank along
424 multi-level piezometer locations (bottom). Sampling point 0 is the inlet and 12 is the outlet.
425 CL refers to the clay liner. Black square is 0.1 m, black circle is 0.4 m and black triangle is
426 0.7 m below the filter surface.

427

428 Fig. 2. Dissolved organic carbon (DOC), HCO_3, dissolved CO_2-C and dissolved CH_4-C at the
429 inlet (black circles) and outlet of the bioreactor (white circles). The influent water was
430 modified with KNO_3 on March 22, 2012.

431

432 Fig. 3. Longitudinal (1-12 sampling points, as per Fig 1) and vertical profiles (at depths of
433 0.7m (box), 0.4 m (triangle), and 0.1 m (cross)) of DOC, dissolved CO_2-C and CH_4-C in the
434 bioreactor before modification of the inlet water with KNO_3 (February 2012 - top row) and
435 after spiking (July 2012). Circle indicates inlet (0) concentrations.
436

437 Fig. 4. Nitrogen (NO_3-N, NH_4-N, dissolved N_2O, DON, N_2/Ar, PN) and P (DRP, DUP and
438 PP) at the inlet (black circles) and outlet of the bioreactor (white circles)). The influent water
439 was modified with KNO_3 on March 22, 2012.

440

441 Fig. 5. Longitudinal (1-12 sampling points, as per Fig 1) and vertical profiles (at depths of
442 0.7m (box), 0.4 m (triangle), and 0.1 m (cross)) of NO_3-N, NH_4-N, N_2/Ar ratios, dissolved
443 N_2O-N, and DRP in the DB before modification of the inlet water with KNO_3 (February 2012
444 - top row) and after spiking (July 2012). Circle indicates inlet (0) concentrations.
445

446 Fig. 6. Example longitudinal N_2O-N, CH_4-C and CO_2-C surface emissions as measured from
447 static chambers at the media surface in the denitrifying bioreactor before NO_3^- spiking
448 (February 2012 - a) and after spiking (June 2012 - b and July 2012 - c).

449

450

451

452

453

454

455

Table 1. Characteristics of the influent water to the denitrifying bioreactor.

	Alkalinity	Nitrate-N	Nitrite-N	Ammonium-N	Dissolved reactive phosphorus	Total phosphorus
	mg L^{-1}	mg L^{-1}	mg L^{-1}	mg L^{-1}	mg L^{-1}	mg L^{-1}
Influent water	223	2.98	Negligible	0.08	0.01	0.07

Table 2. Concentrations of TN, TP and TC within the denitrifying bioreactor used in this study.

	TN	TP	TC
	%	mg L^{-1}	%
WC	0.21	0.014	47
Clay liner	0.11	0.45	0.88
SLS	0.04	1.47	0.25

Table 3. Inlet and outlet mass fluxes (g m^{-2} (surface area) d^{-1}) of NO_3-N, NH_4-N, and DRP in the bioreactor when operated at steady-state, based on data from 14 sampling events. Scenario 1 and 2 considers reductions (positive values) and emissions (negative values) when NO_3-N only is considered (Scenario 1), and when NO_3-N, NH_4-N and DRP are considered (Scenario 2). Weighting Factors applied as per Section 2.5.

	SI Full (g m^{-2} d^{-1})	Cost Damage† (euros m^{-2} y^{-1})	SI 2 Cells
Scenario 1	0.121	2.02	0.112
Scenario 2	-0.00011	1.13	-0.002

† Using costs tabulated in Eory et al. (2013)

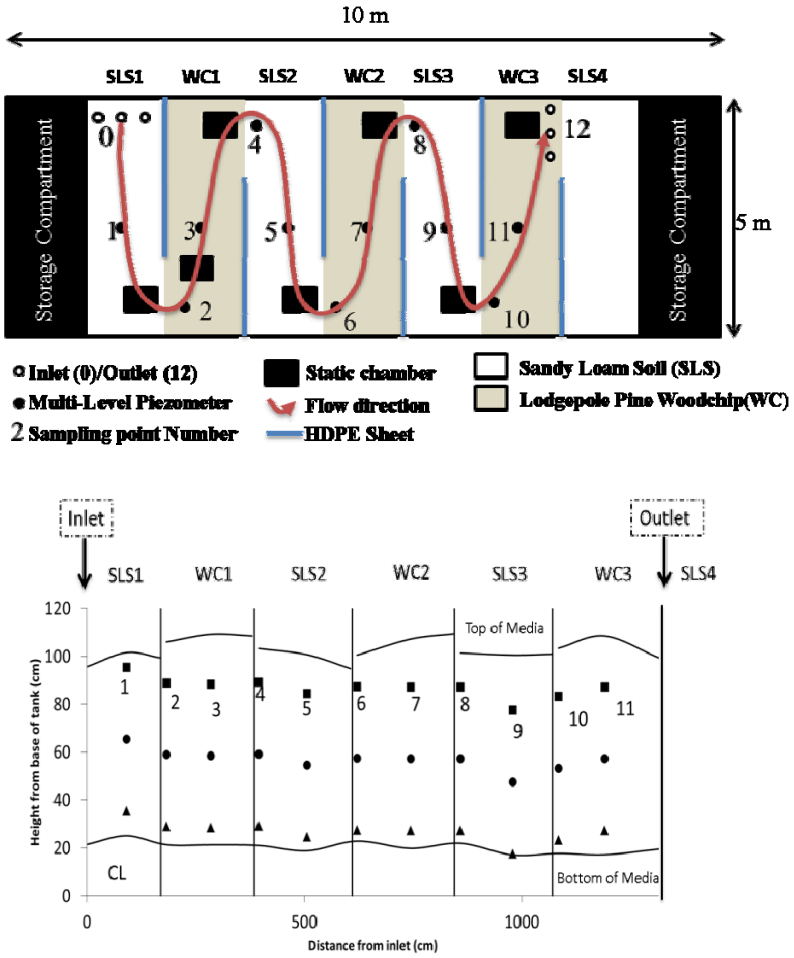

Fig. 1 Schematic top view of the denitrifying bioreactor (top). Cross section of the tank along multi-level piezometer locations (bottom). Sampling point 0 is the inlet and 12 is the outlet. CL refers to the clay liner. Black square is 0.1 m, black circle is 0.4 m and black triangle is 0.7 m below the filter surface.

587

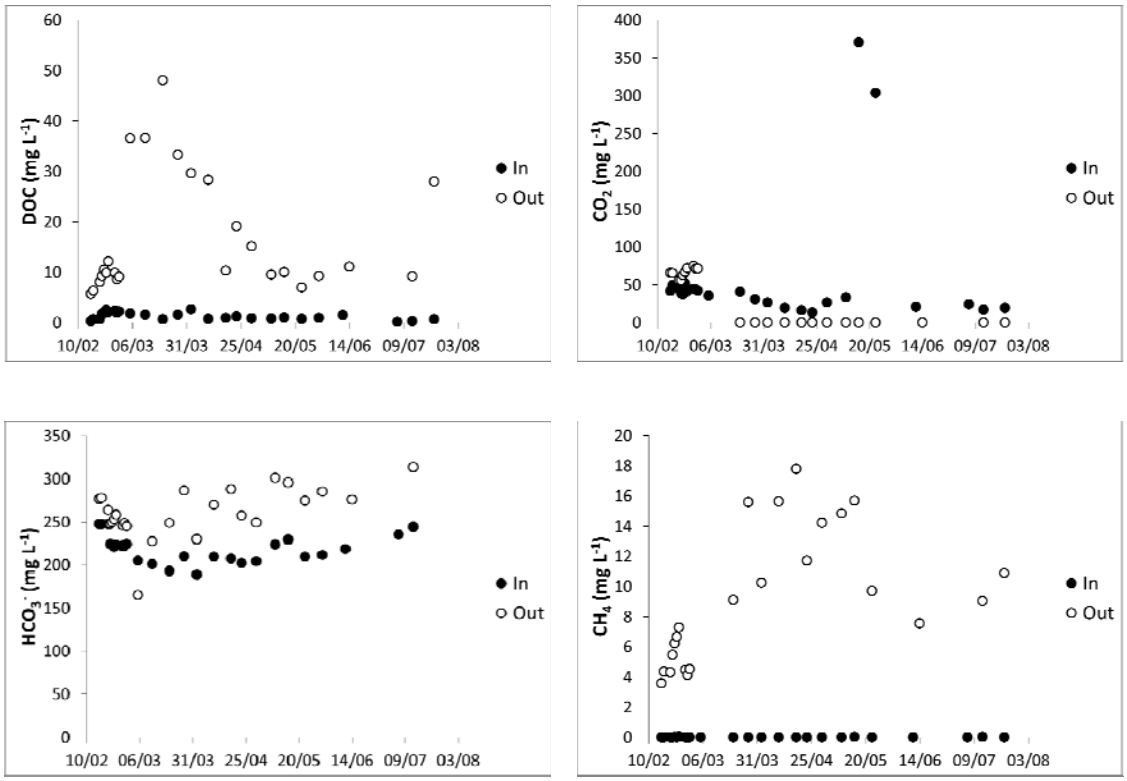

588 Fig. 2. Dissolved organic carbon (DOC), HCO_3, dissolved $CO_{2\text{-}C}$ and dissolved CH_4-C at the
589 inlet (black circles) and outlet of the bioreactor (white circles). The influent water was
590 modified with KNO_3 on March 22, 2012.

591
592
593
594
595
596
597
598
599
600
601
602
603
604
605
606
607
608
609

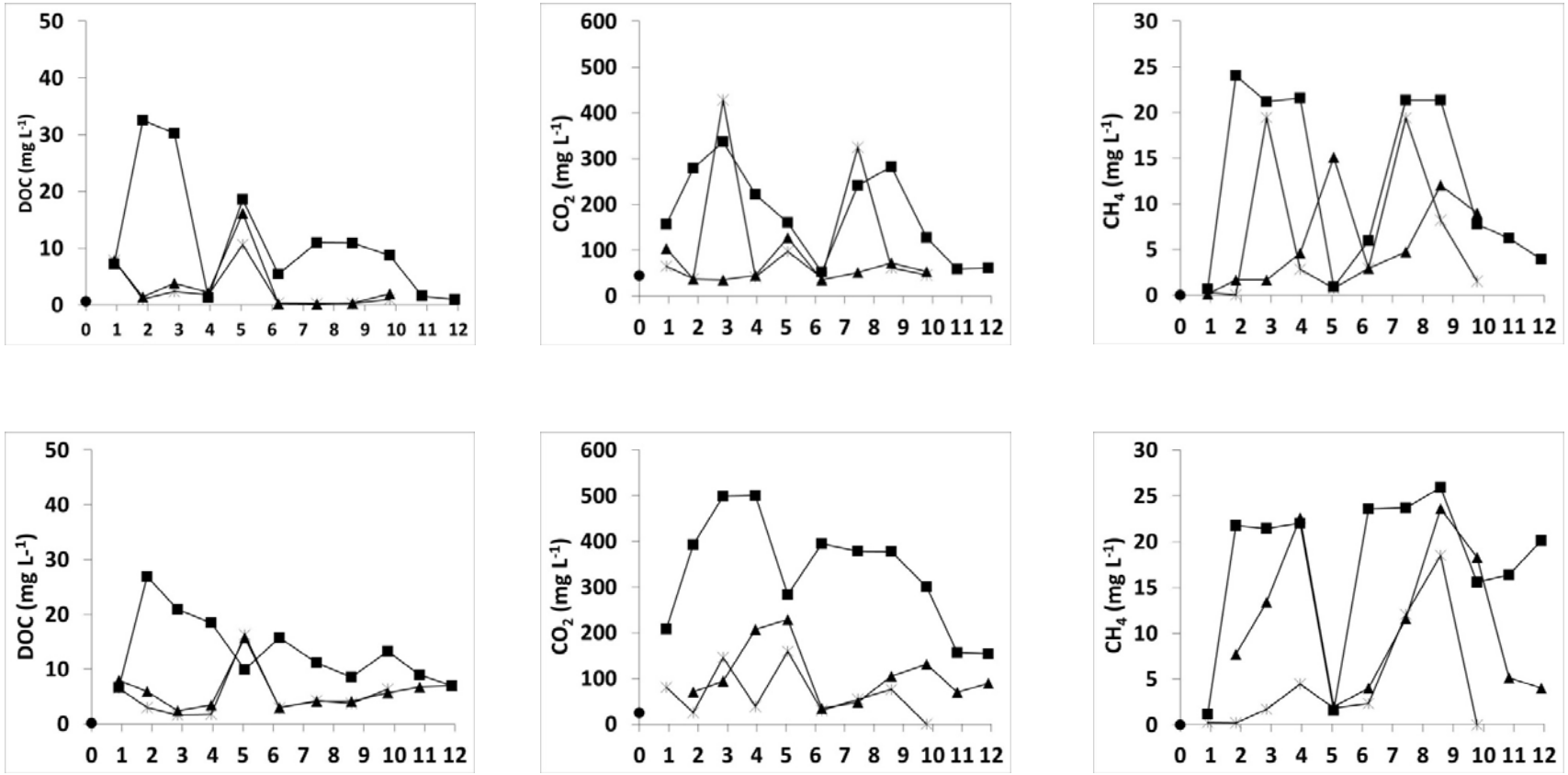

Fig. 3. Longitudinal (1-12 sampling points, as per Fig 1) and vertical profiles (at depths of 0.7m (box), 0.4 m (triangle), and 0.1 m (cross)) of DOC, dissolved $CO_{2\text{-}C}$ and CH_4.C in the bioreactor before modification of the inlet water with KNO_3 (February 2012 - top row) and after spiking (July 2012). Circle indicates inlet (0) concentrations.

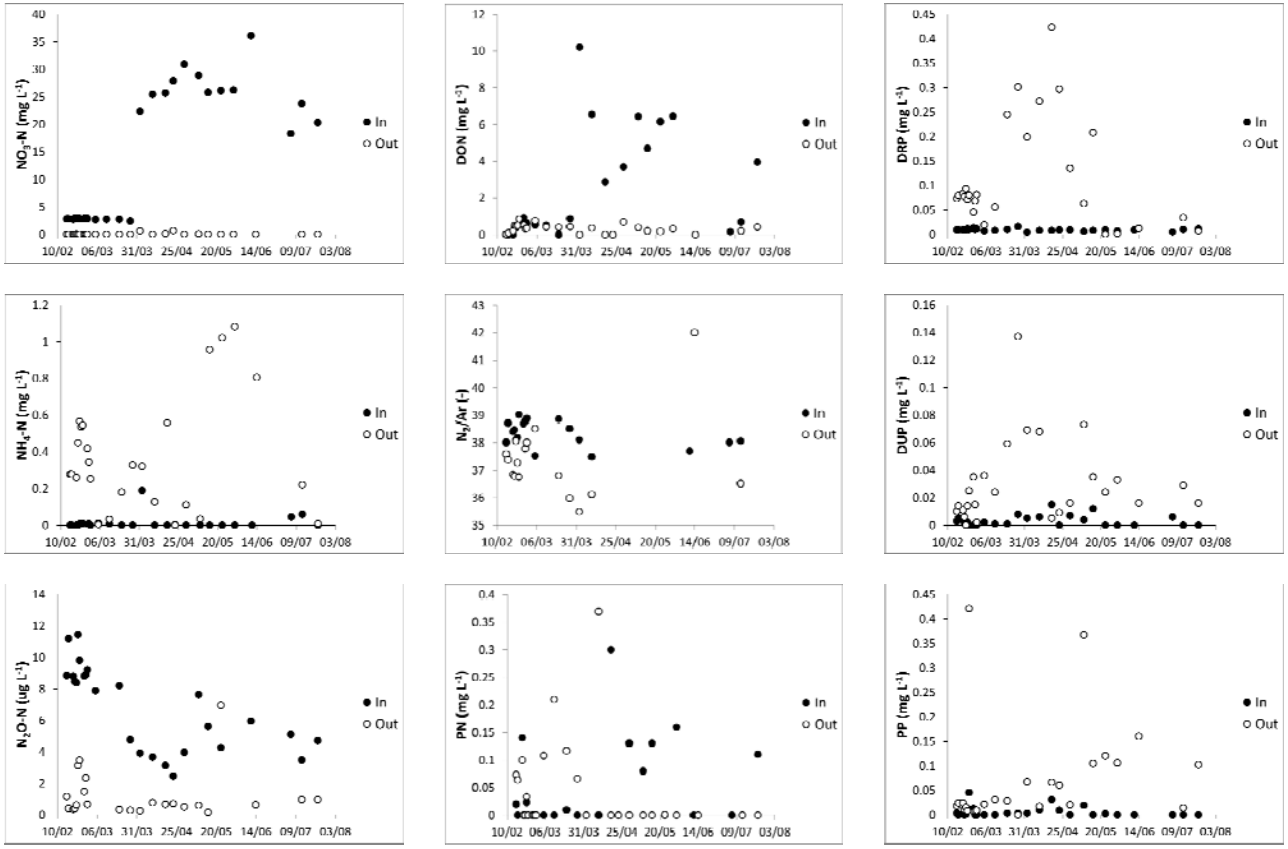

617 Fig. 4. Nitrogen (NO_3-N, NH_4-N, dissolved N_2O, DON, N_2/Ar, PN) and P (DRP, DUP and PP) at the inlet (black circles) and outlet of the
618 bioreactor (white circles)). The influent water was modified with KNO_3 on March 22, 2012.

619
620
621
622

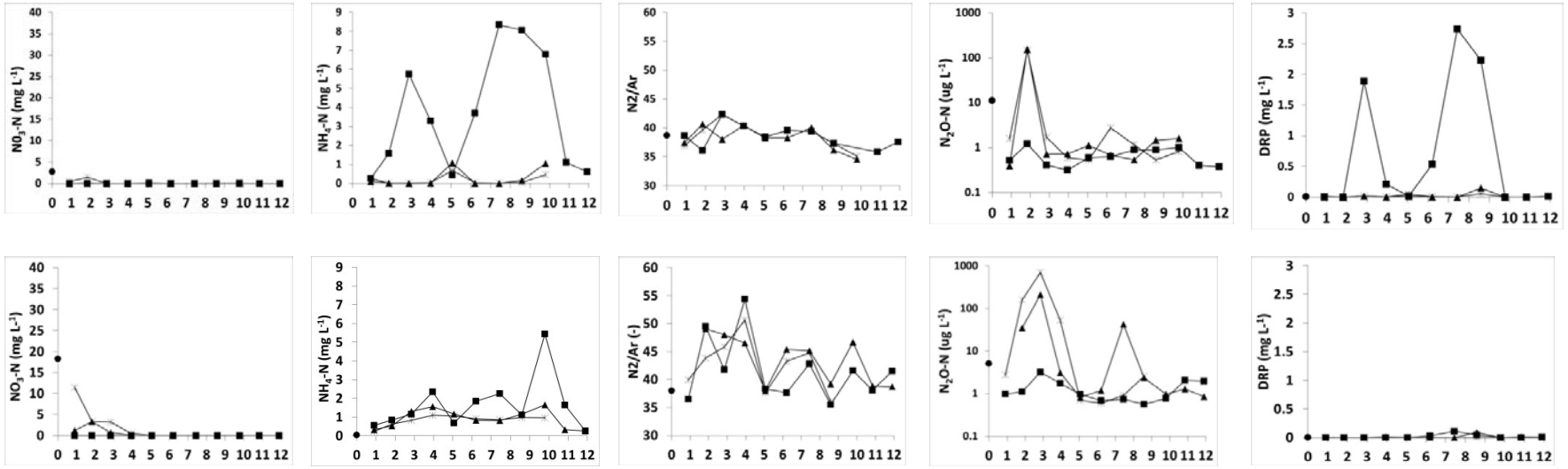

Fig. 5. Longitudinal (1-12 sampling points, as per Fig 1) and vertical profiles (at depths of 0.7m (box), 0.4 m (triangle), and 0.1 m (cross)) of NO_3-N, NH_4-N, N_2/Ar ratios, dissolved N_2O-N, and DRP in the DB before modification of the inlet water with KNO_3 (February 2012 - top row) and after spiking (July 2012). Circle indicates inlet (0) concentrations.

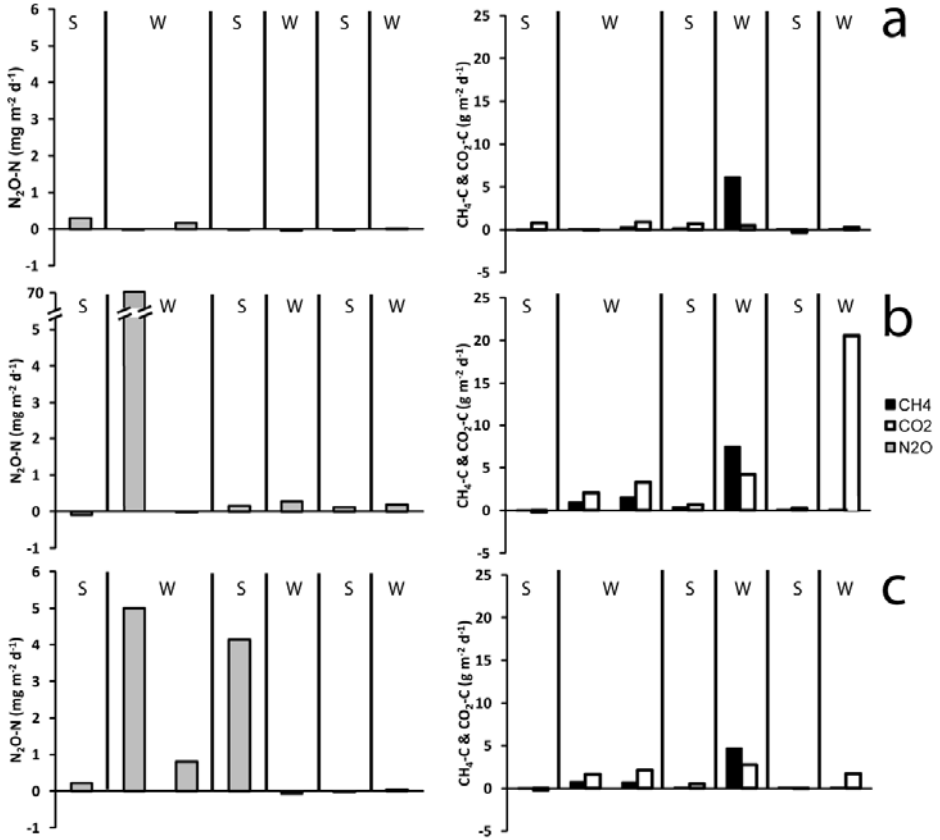

638

639 Fig. 6. Example longitudinal N_2O-N, CH_4-C & CO_2-C surface emissions as measured from static chambers at the media surface in the
640 denitrifying bioreactor before NO_3^- spiking (February 2012 - a) and after spiking (June 2012 - b and July 2012 - c).

641